



Parametric controllable one-way quantum steering induced by four-wave mixing in cavity magnonics

Nan Wang¹, Zhi-Bo Yang^{2,3}, Shi-Yan Li¹, Ting-Ting Dong¹ and Ai-Dong Zhu^{1*}

*Correspondence:
adzhu@ybu.edu.cn

¹Department of Physics, College of Science, Yanbian University, Yanji, Jilin, China

Full list of author information is available at the end of the article

Abstract

Quantum steering plays a crucial role in quantum communication and one-way quantum computation. Here, we study quantum steering between two magnon modes in a cavity-magnonics system by applying a two-photon drive field to the microwave cavity. The two magnon modes are entangled and the one-way steering can be implemented when the four-wave mixing is triggered. Different from most schemes that use the dissipation of the system to control quantum steering, in our scheme the one-way steering can be modulated on demand by adjusting the coherent coupling ratio between the two magnons and the cavity, which provides a flexible and feasible way in experiments. We also reveal that the directionality of quantum steering is related to the mode populations, i.e., the mode with a larger population dominates the steering. Our study has high manipulability and may provide a promising platform for one-way quantum computing and communications based on macroscopic entanglement state.

Keywords: Four-wave mixing; Quantum entanglement; One-way quantum steering

1 Introduction

The light-spin interaction has been studied extensively in recent years which has promoted the rapid development of cavity-magnonics. Magnon, the quanta of collective excitation of spin ensembles in magnetic materials, has many unique characteristics and has attracted much attention in the fields of quantum information processing (QIP). For instance, the higher spin density enabled strong or even ultra-strong coupling between the magnons and photons, namely, a cavity-magnon polaron can be easily formed [1–10], the lower dissipation rate at room temperature makes the cavity-magnon polaron possess good coherence, and the high tunability allows us to observe more phenomena over a wide range of parameters. Due to these advantages the cavity-magnonics has been observed with many interesting applications and phenomena, such as quantum memory [11], quantum transducer [12–17], exceptional point [18, 19] and bistability [20]. The coherent coupling between the photons and magnons plays a crucial role in the construction of QIP platform.

© This is a U.S. Government work and not under copyright protection in the US; foreign copyright protection may apply 2023.
Open Access This article is licensed under a Creative Commons Attribution 4.0 International License, which permits use, sharing, adaptation, distribution and reproduction in any medium or format, as long as you give appropriate credit to the original author(s) and the source, provide a link to the Creative Commons licence, and indicate if changes were made. The images or other third party material in this article are included in the article's Creative Commons licence, unless indicated otherwise in a credit line to the material. If material is not included in the article's Creative Commons licence and your intended use is not permitted by statutory regulation or exceeds the permitted use, you will need to obtain permission directly from the copyright holder. To view a copy of this licence, visit <http://creativecommons.org/licenses/by/4.0/>.

As the key resource of quantum technologies and the most fundamental tests of quantum mechanics [21–23], quantum entanglement plays a crucial role in carrying out the QIP tasks, such as quantum teleportation [24–26], quantum metrology [27], and quantum computing [28–31]. As a strict subset of quantum entanglement, quantum steering was proposed by Schrödinger in response to the famous Einstein-Podolsky-Rosen (EPR) paradox in 1935 [32, 33]. For such “*spooky action-at-a-distance*” phenomenon, the correct explanation is that two observers share pairs of entangled particles, but have completely different abilities to adjust (steer) that particle held by the other one only based on unilateral local measurements. The method of locally measuring one’s own particles to deduce the state of another side is called quantum steering or EPR steering. It is a type of nonclassical correlation that exhibits a strength greater than quantum entanglement [34], yet weaker than Bell nonlocality [35]. Furthermore, the steering has strict directionality and asymmetry, which is particularly evident in one-way steering, i.e., only one side can steer to another side, but not vice versa. The one-way steering effectively breaks the symmetry of controllability, and can be used as an efficient method in quantum manipulation and quantum communications, e.g., one-sided device-independent quantum cryptography [36], quantum secret sharing [37–39], subchannel discrimination [40] and quantum teleportation [41–43].

So far, quantum entanglement and one-way steering have been studied in cavity magnonics by exploiting various methods. The bipartite entanglement and a genuine tripartite entanglement are produced in a magnon-photon-phonon hybrid system by activating the nonlinear magnetostrictive interaction in ferrimagnet, which is accompanied by a cooling process of the phonon mode while the magnon mode is resonant with the anti-Stokes sideband [44–47]. By activating the Kerr nonlinearity of the magnetic material, cavity-magnon entanglement can be generated and then partially transferred to the two magnon modes [48]. Meanwhile, the entanglement caused by the mode overlap between Kittel mode [49] and higher-order magnetostatic mode has also been proposed theoretically [50] by simultaneously activating the self- and cross-Kerr nonlinear effects as well as the four-wave mixing used. Furthermore, the enhanced asymmetric EPR steering and entanglement between two types of magnons on two sublattices have been proposed [51, 52] by introducing a cavity to cool down the magnon modes. More recently, Yang and Guan et al. propose the one-way steering and entanglement in cavity-magnon system and demonstrate that the directivity of EPR steering can be changed by adjusting the ratio of coherent information exchange frequencies [53], and by utilizing the cooperative effect of coherent coupling and dissipative coupling [54], respectively. Inspired by these important advances, here we construct a hybrid cavity-magnonic system to generate bipartite entanglement and one-way steering between two magnons via a process of four-wave mixing. In this system both magnons are coupled to the microwave photons via magnetic dipole interaction, and the microwave cavity is driven by a two-photon drive field (the so-called squeezed drive field). The quantum correlation arises from a four-wave mixing process [55], wherein the two driving photons are absorbed, while the magnon and cavity modes are excited simultaneously. When the four-wave mixing is triggered by manipulating the detuning of two magnon modes to satisfy the frequency matching condition, the bipartite entanglement of subsystem and one-way steering can be realized. Under certain conditions the system parameters are clearly divided into three distinct regions in which the quantum steering between two magnon modes shows completely different unidirectivity,

respectively. In particular, the direction of one-way steering can be regulated not only by the dissipation ratio of the magnons, but also by the coupling strength ratio of two magnon modes to the cavity. This is different from most current contributions in which quantum steering are controlled only by dissipation rates of the magnon modes [56], which cannot be easily adjusted in experimental operation due to the surface roughness, impurities and defects of materials. Hence using the coupling strength to regulate the unidirectionality of quantum steering is more feasible in experimental operations. By analyzing the populations of magnon modes we find that the steering direction is closely dependent on the populations of magnon modes, i.e., the mode with larger population dominates the steering.

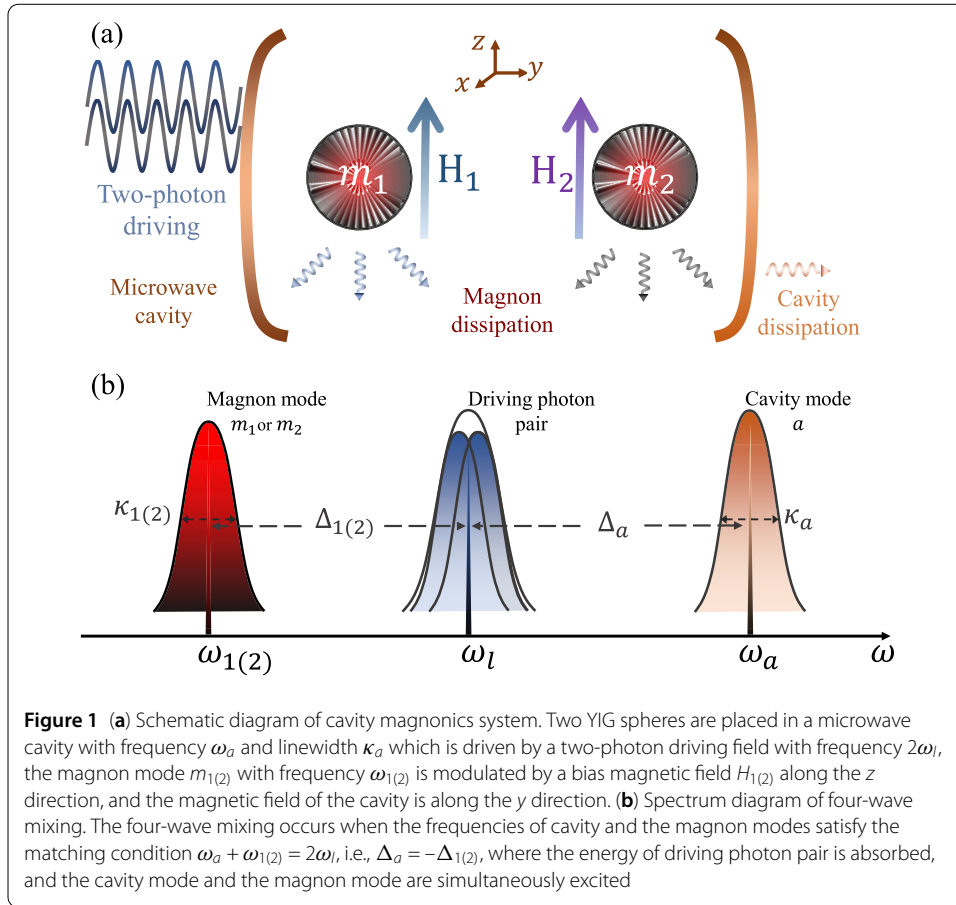
The paper is organized as follows. In Sect. 2, the cavity-magnonics system is constructed and the system dynamics are described by quantum Langevin equations. In Sect. 3, the entanglements between different subsystems are generated based on four-wave mixing, and the characteristics of entanglements are discussed. Also, the physical mechanism of entanglement is analysed by introducing the Bogoliubov modes. In Sect. 4, the implementation of quantum one-way steering is proposed as a controllable manner by regulating the coupling strength ratio between two magnons and the cavity or designing the dissipation ratio of two magnon modes. The connection between one-way steering and the mode populations is revealed. Meanwhile, we demonstrate that the bipartite entanglement and steering are robust to ambient temperature. The feasibility of this system is discussed in Sect. 5, and the conclusions are given in Sect. 6.

2 Model and dynamics

As shown in Fig. 1, we consider a cavity-magnonics system formed by a microwave cavity containing two ferromagnetic yttrium iron garnet (YIG) spheres, where a two-photon drive field is applied to drive the microwave cavity, which results in the squeezing of the cavity field. The two magnon modes are embodied by the collective excitations of a large number of spins in the macroscopic YIG spheres. Furthermore, the strong coupling between the magnon modes and the microwave photons is mediated by the magnetic dipole interaction. We assume that the size of two YIG spheres is smaller enough than the microwave wavelength so that the radiation pressure caused by microwave photons can be well ignored [44, 45, 57, 58]. Under the rotating-wave approximation, the Hamiltonian of the system can be written as ($\hbar = 1$)

$$H = \omega_a a^\dagger a + \sum_{j=1}^2 [\omega_j m_j^\dagger m_j + g_j (a m_j^\dagger + a^\dagger m_j)] + \Omega_0 (a^{\dagger 2} e^{-2i\omega_l t} + a^2 e^{2i\omega_l t}), \quad (1)$$

where O (O^\dagger) ($O = a, m_j$) denotes the annihilation (creation) operators of the cavity mode and j th magnon mode with the corresponding resonance frequency ω_a and ω_j , with $[O, O^\dagger] = 1$. The frequency of magnon mode is determined by the adjustable external bias magnetic field H_j , i.e., $\omega_j = \gamma H_j$ with the gyromagnetic ratio $\gamma/2\pi = 28$ GHz/T. The parameter g_j represents the linear coupling rate between the cavity mode and the j th magnon mode which can be adjusted by varying the direction of the bias field or the position of the YIG spheres inside the microwave cavity [59]. The Rabi frequency Ω_0 represents the coupling strength between the two-photon drive field with frequency $2\omega_l$ and the mi-



microwave cavity mode. In the frame rotating at frequency ω_l , the quantum Langevin equations (QLEs) are given by

$$\begin{aligned} \dot{a} &= -(i\Delta_a + \kappa_a)a - i \sum_{j=1}^2 g_j m_j - 2i\Omega_0 a^\dagger + \sqrt{2\kappa_a} a^{\text{in}}, \\ \dot{m}_j &= -(i\Delta_j + \kappa_j)m_j - ig_j a + \sqrt{2\kappa_j} m_j^{\text{in}}, \end{aligned} \tag{2}$$

where $\Delta_a = \omega_a - \omega_l$, $\Delta_j = \omega_j - \omega_l$ ($j = 1, 2$), κ_a and κ_j denote the dissipation rate of the cavity and magnon mode, respectively, and $O^{\text{in}}(t)$ ($O = a, m_j$) denotes the input noise operator with zero mean of the corresponding mode characterized by the following correlation functions

$$\begin{aligned} \langle O^{\text{in}}(t) O^{\text{in}\dagger}(t') \rangle &= (n_O + 1)\delta(t - t'), \\ \langle O^{\text{in}\dagger}(t) O^{\text{in}}(t') \rangle &= n_O\delta(t - t'), \end{aligned} \tag{3}$$

for the equilibrium mean thermal number of the corresponding mode $n_O = [\exp(\hbar\omega_O / K_B T) - 1]^{-1}$ with the ambient temperature T and Boltzmann constant K_B . Since the microwave cavity is strongly driven by a two-photon drive field, the photon amplitude $|\langle a \rangle| \gg 1$. Meanwhile, the magnon modes also have large amplitudes due to the beam-splitter interactions between the cavity photons and the magnon modes, i.e., $|\langle m_j \rangle| \gg 1$.

By linearizing the dynamics of the system around the steady-state values, each operator can be written as $O = \langle O \rangle + \delta O$. Thus the linearized QLEs of the quantum fluctuations are obtained as

$$\begin{aligned} \delta \dot{a} &= -(i\Delta_a + \kappa_a)\delta a - i \sum_{j=1}^2 g_j \delta m_j - 2i\Omega_0 \delta a^\dagger + \sqrt{2\kappa_a} \delta a^{\text{in}}, \\ \delta \dot{m}_j &= -(i\Delta_j + \kappa_j)\delta m_j - i g_j \delta a + \sqrt{2\kappa_j} \delta m_j^{\text{in}}. \end{aligned} \tag{4}$$

By defining the fluctuations of quadratures $\delta X_a = (\delta a + \delta a^\dagger)/\sqrt{2}$, $\delta Y_a = i(\delta a^\dagger - \delta a)/\sqrt{2}$, $\delta X_j = (\delta m_j + \delta m_j^\dagger)/\sqrt{2}$, $\delta Y_j = i(\delta m_j^\dagger - \delta m_j)/\sqrt{2}$, the linearized QLEs can be rewritten in a compact matrix form

$$\dot{u}(t) = Au(t) + n(t), \tag{5}$$

with $u(t) = [\delta X_a(t), \delta Y_a(t), \delta X_1(t), \delta Y_1(t), \delta X_2(t), \delta Y_2(t)]^T$, and $n(t) = [\sqrt{2\kappa_a}X_a^{\text{in}}(t), \sqrt{2\kappa_a}Y_a^{\text{in}}(t), \sqrt{2\kappa_1}X_1^{\text{in}}(t), \sqrt{2\kappa_1}Y_1^{\text{in}}(t), \sqrt{2\kappa_2}X_2^{\text{in}}(t), \sqrt{2\kappa_2}Y_2^{\text{in}}(t)]^T$ is the vector of input noises and the superscript ‘T’ represents the transpose. The drift matrix A is written as

$$A = \begin{pmatrix} -\kappa_a & \Delta_a - 2\Omega_0 & 0 & g_1 & 0 & g_2 \\ -\Delta_a - 2\Omega_0 & -\kappa_a & -g_1 & 0 & -g_2 & 0 \\ 0 & g_1 & -\kappa_1 & \Delta_1 & 0 & 0 \\ -g_1 & 0 & -\Delta_1 & -\kappa_1 & 0 & 0 \\ 0 & g_2 & 0 & 0 & -\kappa_2 & \Delta_2 \\ -g_2 & 0 & 0 & 0 & -\Delta_2 & -\kappa_2 \end{pmatrix}. \tag{6}$$

Owing to the linearized dynamics and the Gaussian nature of quantum noises, quantum fluctuation of a steady-state system is a continuous variable three-mode Gaussian state, which can be completely characterized by a 6×6 covariance matrix (CM) \mathcal{V} defined as $2\mathcal{V}_{ij}(t, t') = \langle u_i(t)u_j(t') + u_j(t')u_i(t) \rangle$. The stationary CM \mathcal{V} can be obtained by solving the Lyapunov equation [60]

$$A\mathcal{V} + \mathcal{V}A^T = -D, \tag{7}$$

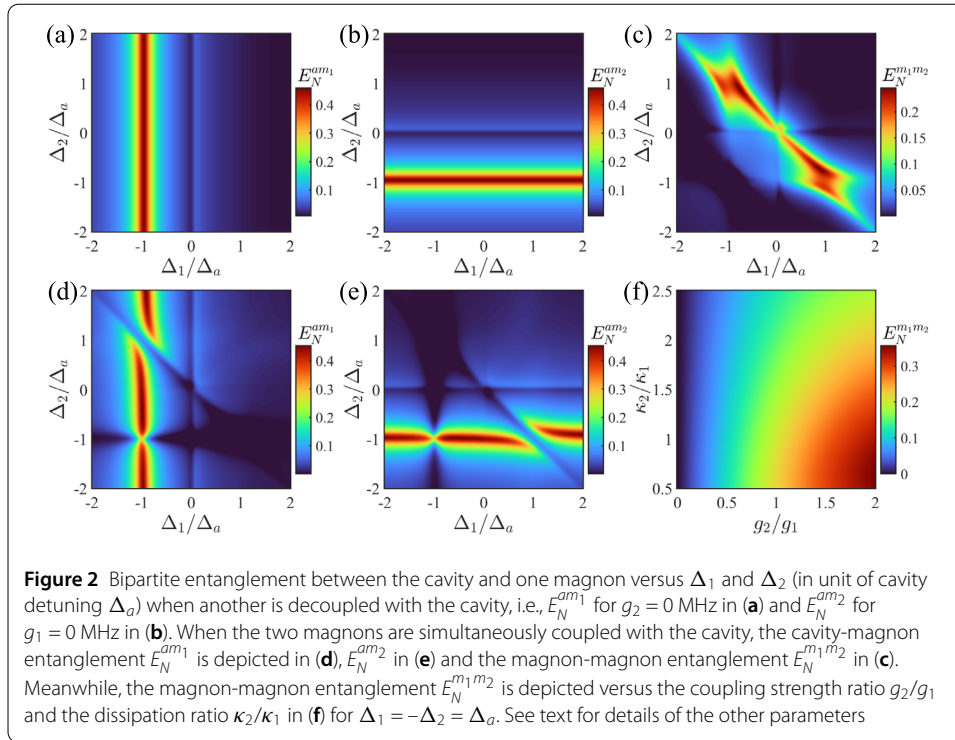
where $D = \text{diag}[\kappa_a(2n_a + 1), \kappa_a(2n_a + 1), \kappa_1(2n_{m_1} + 1), \kappa_1(2n_{m_1} + 1), \kappa_2(2n_{m_2} + 1), \kappa_2(2n_{m_2} + 1)]$ is the diffusion matrix defined by $2D_{ij}\delta(t - t') = \langle n_i(t)n_j(t') + n_j(t')n_i(t) \rangle$.

Next we study the entanglement and quantum steering of the two magnon modes by using the CM \mathcal{V} .

3 Bipartite entanglement generated via four-wave mixing

We adopt the logarithmic negativity E_N to quantify the quantum entanglement [61–64], which can be computed from the reduced 4×4 CM $\tilde{\mathcal{V}}$ for any two modes

$$\tilde{\mathcal{V}} = \begin{pmatrix} \mathcal{V}_1 & \mathcal{V}_3 \\ \mathcal{V}_3^T & \mathcal{V}_2 \end{pmatrix}, \tag{8}$$



where \mathcal{V}_1 , \mathcal{V}_2 and \mathcal{V}_3 are 2×2 sub-block of matrices of $\tilde{\mathcal{V}}$. The logarithmic negativity for entanglement of two modes is defined as

$$E_N \equiv \max[0, -\ln 2\nu], \quad (9)$$

where $\nu = \sqrt{\mathcal{E} - (\mathcal{E}^2 - 4\mathcal{R})^{1/2}}/\sqrt{2}$ with $\mathcal{E} = \mathcal{R}_1 + \mathcal{R}_2 - 2\mathcal{R}_3$, $\mathcal{R}_1 = \det \mathcal{V}_1$, $\mathcal{R}_2 = \det \mathcal{V}_2$, $\mathcal{R}_3 = \det \mathcal{V}_3$ and $\mathcal{R} = \det \tilde{\mathcal{V}}$ being symplectic invariants.

The entanglement characteristics of the system in steady state is guaranteed by the eigenvalues (negative real parts) of the drift matrix A (i.e., $|A - \lambda I| = 0$). On this premise, the following feasible experimental parameters in Ref. [50] can be used: $\Delta_a/2\pi = 200$ MHz, $g_1/2\pi = g_2/2\pi = 42$ MHz, $\kappa_a/2\pi = 6$ MHz, $\kappa_1/2\pi = \kappa_2/2\pi = 12$ MHz and $\Omega_0/2\pi = 30$ MHz. The cavity-magnon entanglements $E_N^{am_1}$ and $E_N^{am_2}$ are shown in Figs. 2(a) and 2(b), where only one magnon mode m_1 or m_2 is considered, i.e., $g_1 \neq 0$, $g_2 = 0$ in the former and $g_1 = 0$, $g_2 \neq 0$ in the latter. We can see that the maximum entanglement occurs at $\Delta_1 = -\Delta_a$ for $E_N^{am_1}$ and at $\Delta_2 = -\Delta_a$ for $E_N^{am_2}$, exactly corresponding to the condition of four-wave mixing $\omega_a + \omega_{1(2)} = 2\omega_l$. Due to the two-photon drive field, the energy of one photon of the driving photon pair is absorbed to excite the magnon mode with detuning $\Delta_1/2\pi = -200$ MHz (or $\Delta_2/2\pi = -200$ MHz), and the remaining energy is simultaneously scattered into the cavity resonance with detuning $\Delta_a/2\pi = 200$ MHz. The above frequency matching condition is the key for generating entanglements. When the two magnon modes are simultaneously coupled to the cavity mode, i.e., $g_1 \neq 0$ and $g_2 \neq 0$, the bipartite entanglement of the hybrid cavity magnonic system presents a different phenomenon, as shown in the Figs. 2(d) and 2(e). A breaking point at $\Delta_1 = -\Delta_a = -\Delta_2$ appears for entanglement $E_N^{am_1}$ in Fig. 2(d), and $\Delta_1 = \Delta_a = -\Delta_2$ appears for $E_N^{am_2}$ in Fig. 2(e). Meanwhile, the magnon-magnon entanglement degree $E_N^{m_1m_2}$ increases significantly in these

two breaking points as seen in the Fig. 2(c). This type of phenomenon is also observed in the magnetostriction-induced stationary entanglement between two microwave fields [46], and can be enhanced by using an optical parametric amplifier [65]. By comparing the Fig. 2(c) with 2(d) and 2(e), we can clearly see that the cavity-magnon entanglement is transferred to that between the two magnon modes via the beam splitter interactions. In the Fig. 2(f), magnon-magnon entanglement $E_N^{m_1 m_2}$ is shown as a function of the cavity-magnon coupling ratio g_2/g_1 and the dissipation ratio of magnon modes κ_2/κ_1 . We can see that the bipartite entanglement $E_N^{m_1 m_2}$ increases gradually to its maximum value as the increasing of the coupling ratio g_2/g_1 for a fixed dissipation ratio κ_2/κ_1 . On the contrary, it decreases gradually as the magnon dissipation ratio κ_2/κ_1 increases when the coupling ratio g_2/g_1 is fixed. This indicates the bipartite entanglement between two magnons can be controlled with either the dissipation ratio of two magnons or coupling ratio between two magnon-cavity interactions.

To better understand the physical mechanism of entanglement between the subsystems, we diagonalize the Hamiltonian by introducing Bogoliubov modes [66, 67] $\alpha = S^\dagger(r)aS(r) = a \cosh r + a^\dagger \sinh r$, $\alpha^\dagger = S^\dagger(r)a^\dagger S(r) = a^\dagger \cosh r + a \sinh r$, where r denotes the squeezing coefficient, $\tanh 2r = 2\Omega_0/\Delta_a$, and α and α^\dagger satisfy the bosonic-commutation relation. In the frame rotating at frequency ω_l , the Hamiltonian Eq. (1) becomes

$$\mathcal{H} = \Delta_\alpha \alpha^\dagger \alpha + \sum_{j=1}^2 [\Delta_j m_j^\dagger m_j + g_j^{cos} (\alpha m_j^\dagger + \alpha^\dagger m_j) + g_j^{sin} (\alpha^\dagger m_j^\dagger + \alpha m_j)], \tag{10}$$

with $\Delta_\alpha = \sqrt{\Delta_a^2 - 4\Omega_0^2}$, $g_j^{cos} = g_j \cosh r$ and $g_j^{sin} = -g_j \sinh r$. The Eq. (10) shows that $\Delta_\alpha = -\Delta_j$ is the optimal detuning for the cavity-magnon entanglement due to the cavity-magnon squeezing term $(\alpha^\dagger m_j^\dagger + \alpha m_j)$, which corresponds exactly to the frequency matching condition of four-wave mixing in Fig. 1(b). Meanwhile, the state-swap interaction between the cavity and magnon modes is also enhanced due to the term $g_j^{cos} > g_j$ for $r > 0$. The cavity-magnon entanglement is originated from the parametric-type interaction (two-mode-squeezing term) caused by two-photon drive field. While the magnon-magnon entanglement results from the entanglement transfer caused by the state-swap interaction, as shown in the Fig. 2.

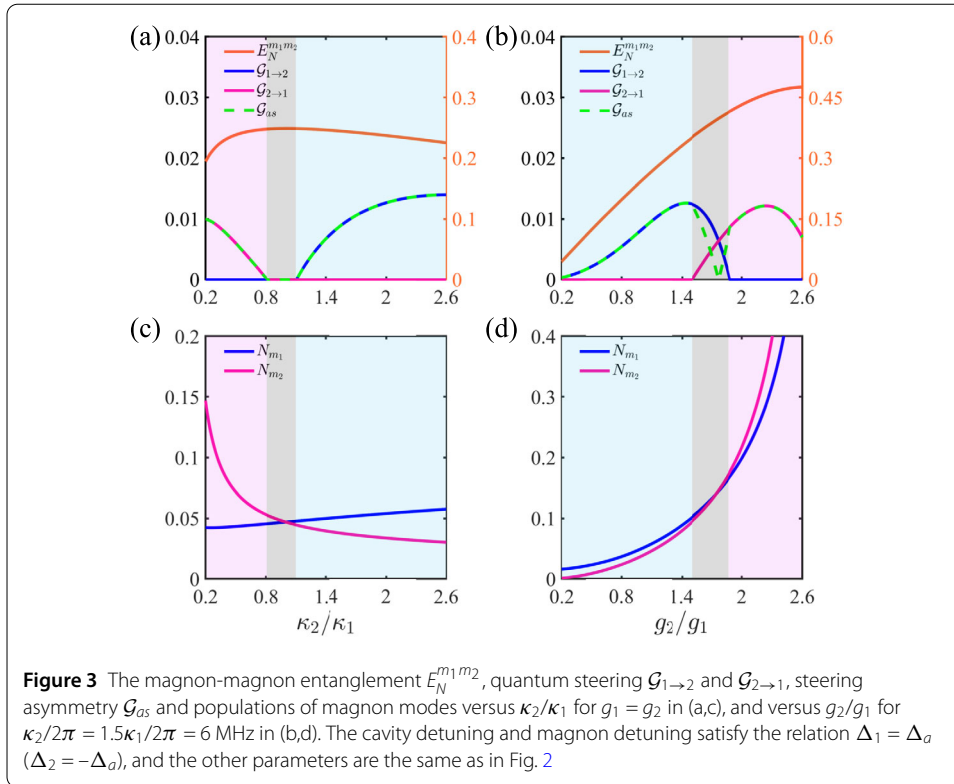
4 Parametric controllable one-way steering

Now we turn to the generation and manipulation of one-way steering. The Gaussian steering can be obtained through Gaussian measurements on one of the two magnon modes, which is given by [68]

$$\begin{aligned} \mathcal{G}_{1 \rightarrow 2} &= \max \left[0, \frac{1}{2} \ln \frac{\mathcal{R}_1}{4\mathcal{R}} \right], \\ \mathcal{G}_{2 \rightarrow 1} &= \max \left[0, \frac{1}{2} \ln \frac{\mathcal{R}_2}{4\mathcal{R}} \right]. \end{aligned} \tag{11}$$

To assess the degree of asymmetry in the steerability of the two magnon modes, we define the Gaussian steering asymmetry as

$$\mathcal{G}_{as} = |\mathcal{G}_{1 \rightarrow 2} - \mathcal{G}_{2 \rightarrow 1}|. \tag{12}$$



To better explain the directionality of the one-way steering between two magnon modes, we introduce the mode populations, i.e., the final mean magnon numbers, which can be obtained from the relation

$$N_{m_j} = \frac{1}{2} [\langle \delta X_j^2 \rangle + \langle \delta Y_j^2 \rangle - 1], \tag{13}$$

with $j = 1, 2$ corresponding to the two magnons, respectively.

In most current studies, the magnon dissipation rate is often used as a main means to regulate the direction of one-way steering [56], which will not only introduce additional dissipation or noise, reducing the entanglement and steering degree, but also increase the difficulty of experimental operations. Since the dissipation of magnon mode is only related to the surface roughness, impurities and defects of YIG sphere, it cannot be flexibly adjusted in operations. However, as we will see later that in our current study the one-way steering can be regulated on demand with the coherence coupling strength ratio between the two magnons and the cavity, which can be performed by changing the position of the YIG spheres in the cavity field. This provides great convenience for experimental operations.

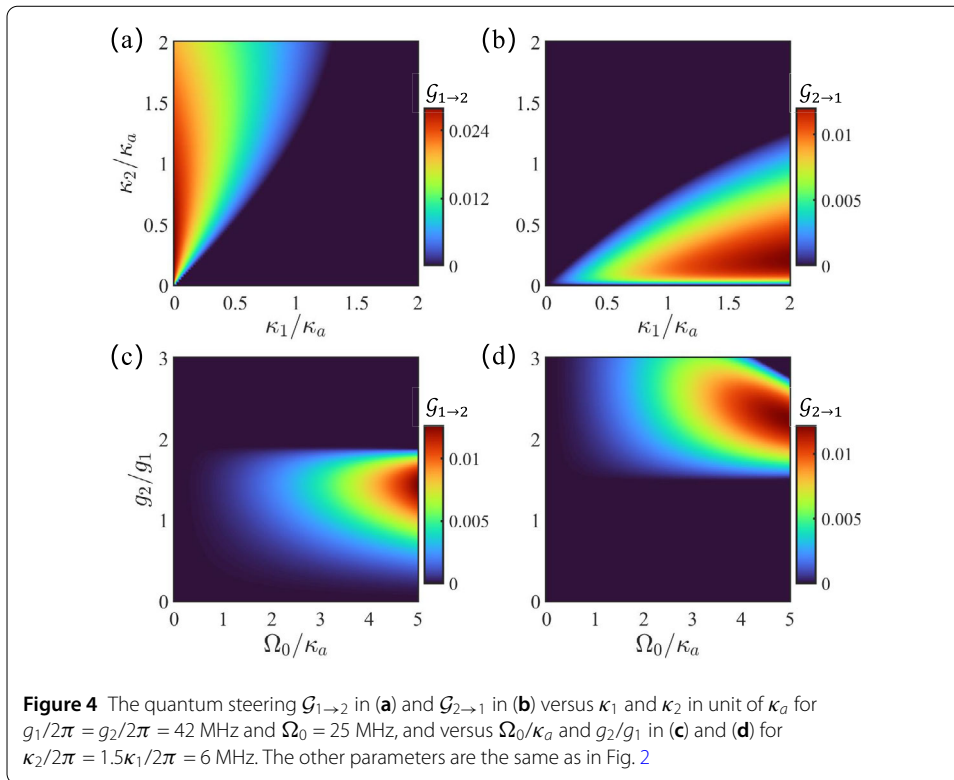
From the Eq. (9) and Eqs. (11)–(13), the bipartite entanglement, quantum steering, steering asymmetry and populations of the magnon modes are described as the functions of dissipation ratio κ_2/κ_1 or coupling strength ratio g_2/g_1 of the two magnon modes in Fig. 3. In order to illustrate the controllability of quantum steering more intuitively, we have marked the one-way steering region of $\mathcal{G}_{1 \rightarrow 2}$ ($\mathcal{G}_{2 \rightarrow 1}$) in blue (purple), the two-way steering region in white, and steering-free region in grey. As shown in Fig. 3(a), since the interactions between the cavity and two magnon modes are nearly balanced for equivalent cavity-

magnon coupling strengths $g_2/g_1 = 1$ and dissipation rates $\kappa_2/\kappa_1 = 1$, a narrow steering-free region appears in the range $0.8 < \kappa_2/\kappa_1 < 1.2$ centered on this balance point. On both sides of this region, the balance of cavity-magnon interactions is broken due to the different dissipation rates of the two magnon modes, thus the one-way steering appears, i.e., on the left side ($\kappa_2/\kappa_1 < 0.8$) $\mathcal{G}_{2 \rightarrow 1} \neq 0$, $\mathcal{G}_{1 \rightarrow 2} = 0$ and reversely on the right side ($\kappa_2/\kappa_1 > 1.2$). We can observe that on the left side the one-way steering $\mathcal{G}_{2 \rightarrow 1}$ (purple line in purple area) decreases with the increase of dissipation ratio κ_2/κ_1 until vanishes at $\kappa_2/\kappa_1 \simeq 0.8$, while on the right side $\mathcal{G}_{1 \rightarrow 2}$ begin to increase gradually from the point $\kappa_2/\kappa_1 \simeq 1.2$. Obviously, the steering-free region is a transition zone between two different directions of one-way steering, within which the two magnons is always entangled. Therefore, the dissipation ratio of the two magnon modes can be used as a “double-throw switch” of quantum steering under a fixed coupling ratio g_2/g_1 , i.e., it switches the one-way steering between $\mathcal{G}_{2 \rightarrow 1}$ and $\mathcal{G}_{1 \rightarrow 2}$, and turn off in the steering-free region.

However, as mentioned above that the dissipation ratio of the magnons cannot be conveniently adjusted in operations. While the cavity-magnon coupling strength can be flexibly controlled in the cavity-magnonics system by adjusting the external bias magnetic field or arranging the position of YIG spheres in the cavity [53]. When the dissipation ratio is fixed at an appropriate value, e.g., $\kappa_2/\kappa_1 = 1.5$ as shown in Fig. 3(b), the steering can be performed in a controllable manner by adjusting the coupling strength ratio. We can see that steering $\mathcal{G}_{1 \rightarrow 2}$ (blue line in blue region) gradually increases as the increase of g_2/g_1 . Nevertheless, after reaching a peak around $g_2/g_1 \approx 1.5$, the steering $\mathcal{G}_{2 \rightarrow 1}$ increases rapidly and creates a competitive relationship with $\mathcal{G}_{1 \rightarrow 2}$ in the white region. In other words, the two-way steering region $1.5 < g_2/g_1 < 1.9$ appears, which is a competition zone of two directions of quantum steering. With the increase of g_2/g_1 , $\mathcal{G}_{2 \rightarrow 1}$ gradually dominates over $\mathcal{G}_{1 \rightarrow 2}$, until the transition to the one-way steering region of $\mathcal{G}_{2 \rightarrow 1}$. From the perspective of cavity-magnon couplings, the cavity magnonics system is completely symmetric when both the dissipation ratio and the coupling strength ratio are close to 1, thus no quantum steering exists between the two magnons despite entanglement. However, two ways can be used to break the balance of interaction, via the dissipation ratio or coupling strength ratio, and thus asymmetric steering can be realized. A mode with a higher dissipation rate requires a greater coupling strength to maintain this balance of interactions, i.e., more frequent coherent information exchange with the cavity than a mode with a lower dissipation rate. Therefore, in case of a fixed coupling strength ratio, the party with higher dissipation rate is passive in steerability. Meanwhile, in case of a fixed dissipation ratio, the party with the greater coherent coupling with the cavity is dominant over the other one in steerability.

The directionality of quantum steering is analyzed in terms of the mode populations in Figs. 3(c) and 3(d). Compare 3(a) with 3(c), and 3(b) with 3(d), the correlation is clearly shown between the steering direction and the mode populations. The purple area for $N_{m_2} > N_{m_1}$ corresponds to one-way steering region of $\mathcal{G}_{2 \rightarrow 1}$, and the blue area for $N_{m_1} > N_{m_2}$ corresponds to the one-way steering region of $\mathcal{G}_{1 \rightarrow 2}$. In the steering-free and competition region the populations of two magnon modes are nearly equal. One mode with a larger population has dominance in steering over the other one.

The above results show that the directionality of one-way quantum steering can be performed in a parametric controllable manner. Especially, the magnon populations can be changed by modulating the cavity-magnon coupling ratio under an appropriate dissipa-

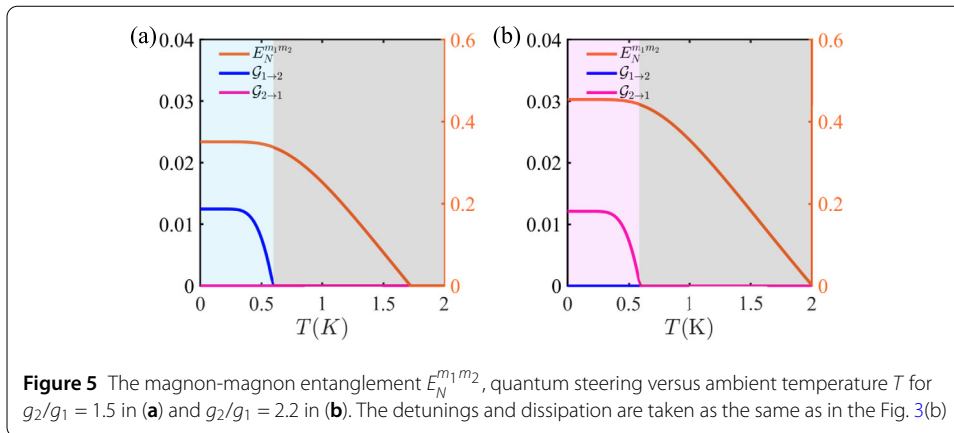


tion ratio of two magnon modes, which consequently causes the change of steering direction. Undoubtedly, this provides another flexible path to manipulate quantum steering.

In Figs. 4(a) and 4(b), the quantum steering $\mathcal{G}_{1 \rightarrow 2}$ and $\mathcal{G}_{2 \rightarrow 1}$ are depicted, respectively, as a function of the magnon dissipation rates in unit of the cavity decay rate. As we can see in the Fig. 4(a), the steering $\mathcal{G}_{1 \rightarrow 2}$ reaches its maximum at $\kappa_1 = 0$, and then decreases with the increase of κ_1 for a fixed κ_2 . Similarly, in the Fig. 4(b) the steering $\mathcal{G}_{2 \rightarrow 1}$ reaches its maximum at $\kappa_2 = 0$. Then $\mathcal{G}_{2 \rightarrow 1}$ decreases with the increase of κ_2 for a fixed κ_1 . The Fig. 4(a) and 4(b) clearly show that the steering in opposite directions $\mathcal{G}_{2 \rightarrow 1}$ and $\mathcal{G}_{1 \rightarrow 2}$ appear in completely different parameter areas.

In Figs. 4(c) and 4(d), $\mathcal{G}_{1 \rightarrow 2}$ and $\mathcal{G}_{2 \rightarrow 1}$ are described, respectively, versus the drive strength Ω_0 (in unit κ_a) and the coherent coupling ratio g_2/g_1 . We can see that the steering degree increases gradually as the drive strength Ω_0 increases. However, the directionality of steering can be changed by increasing the cavity-magnon coupling strength ratio, i.e., with the increasing of g_2/g_1 , the steering between two magnons will transits from one-way steering region of $\mathcal{G}_{1 \rightarrow 2}$ to two-way steering region and then to one-way steering region of $\mathcal{G}_{2 \rightarrow 1}$. This is consistent with the description in Fig. 3.

Finally, the maximum values of $\mathcal{G}_{1 \rightarrow 2}$ and $\mathcal{G}_{2 \rightarrow 1}$ in Fig. 3(b) as well as the entanglement $E_N^{m_1 m_2}$ are described for the ambient temperature T as shown in Fig. 5(a) and 5(b). It is evident that the entanglement and one-way steering between two magnons exhibit robustness within a certain temperature range. Specifically, for the taken coupling strength ratios $g_2/g_1 = 1.5$, the entanglement exists until 1.6 K, and the one-way steering $\mathcal{G}_{1 \rightarrow 2}$ remains below 0.6 K, as shown in Fig. 5(a). Whereas the increasing in g_2/g_1 results in the enhancement of the robustness of entanglement, as shown in Fig. 5(b), where the entanglement exists until 2 K for $g_2/g_1 = 2.2$. When magnon coupling strength ratio and dis-



sipation ratio are fixed both the entanglement and quantum steering decrease with the increase of ambient temperature T .

5 Discussions

In our present system two YIG spheres are mounted in a microwave cavity driven by a two-photon drive field. The purpose of using spherical objects is to avoid the influences of inhomogeneous demagnetization field. Meanwhile, a nearly uniform microwave field is used to avoid the interaction of YIG spheres with other unnecessary magnetostatic modes [18]. Typically, the fabrication of single-crystal YIG sphere is limited to a diameter range of 200–1000 μm [5]. However, the volume of YIG sphere is positively correlated with the cavity-magnon coupling strength, while negatively correlated with the Kerr nonlinear coefficient [69]. Therefore, in order to optimize the coupling strength while minimizing nonlinearity, we select a 250 μm diameter YIG sphere [44]. The construction of four-wave mixing and the generation of optimal magnon-magnon entanglement can be achieved by modulating the bias magnetic field, wherein the frequency of the cavity TE_{120} mode is fixed at $\omega_a/2\pi = 10$ GHz. When the frequency of one of the two magnon modes is taken as $\omega_j/2\pi = 9.6$ GHz (corresponding to $\Delta_j = -\Delta_a$ and $H_j = 0.343$ T), and the frequency of two-photon drive field satisfies $2\omega_l/2\pi = 19.6$ GHz, the four-wave mixing occurs. This indicates that four-wave mixing process can be triggered by either of the two magnon modes that satisfy the frequency matching condition $2\omega_l = \omega_a + \omega_j$. If the detuning of magnon modes satisfies the relation $\Delta_1 = \Delta_a$ & $\Delta_2 = -\Delta_a$ by tuning the bias fields as $H_1(H_2) = 0.357$ T (0.343 T), or the relation $\Delta_1 = -\Delta_a$ & $\Delta_2 = \Delta_a$ by adjusting the bias fields as $H_1(H_2) = 0.343$ T (0.357 T), the maximum magnon-magnon entanglement can be generated, corresponding to the situation in Fig. 2(c).

In order to regulate the direction of one-way steering on demand with the cavity-magnon coupling strength ratio, the relation between cavity-magnon coupling rates and the location of YIG spheres in the cavity can be used according to the methods in Refs. [11, 18]. In detail, one of the two YIG spheres is firstly fixed, the other one is glued on a thin wooden rod to change its position in microwave magnetic field of the TE_{120} mode along the y direction by using a position adjustment stage. This method is more flexible in operations than the method using the dissipation ratio of the magnons. Once a YIG sphere has been prepared its dissipation rate is determined and cannot be easily adjusted during the experimental operations. But the detection of the one-way steering is considered

as a method to determine the dissipation rate of the magnon mode [52]. The bipartite entanglement and quantum steering can be demonstrated by measuring the covariance matrix via balanced homodyne detection [60]. Coupling magnon mode to an additional weak microwave field with a dissipation rate greater than that of the magnon modes via a beamsplitter-type interaction, the quadratures of magnon mode can be measured. By probing the output of the auxiliary cavity, the magnon state can be read out [70, 71]. These experimentally feasible technologies can support our current scheme.

6 Conclusion

We have constructed a cavity-magnonics system by placing two identical YIG spheres in a microwave cavity to implement quantum entanglement and one-way steering between two magnons by using a two-photon drive field to trigger a four-wave mixing. The entanglement of subsystem is originated from the nonlinearity caused by the four-wave mixing process. When the beamsplitter interaction between two magnons and the cavity is balanced, although the two magnon modes are entangled, no quantum steering is generated between them. However, the one-way steering occurs once this balance is broken. It can be completed not only by designing the dissipation ratio between the two magnons but also by regulating the coherent coupling strength ratio between the two magnons and the cavity. Especially, adjusting the coupling strength ratio is a method more flexible and convenient in operations for realizing the optimal one-way steering in different directions. We find that the steering directionality is related with the mode populations, i.e., the mode with a higher population always dominates quantum steering. Both the quantum entanglement and one-way steering are robust to ambient temperature. Our results demonstrate a feasible way for coherently manipulating entanglement and one-way steering in cavity-magnonics, which provides a macroscopic QIP platform for quantum key distribution, quantum secret sharing, one-way quantum computing.

Funding

This work is supported by the National Natural Science Foundation of China under Grant No. 12264051.

Abbreviations

QIP, Quantum information processing; EPR, Einstein-Podolsky-Rosen; YIG, Yttrium iron garnet; QLEs, Quantum Langevin equations; CM, Covariance matrix.

Availability of data and materials

Not applicable. For all requests relating to the paper, please contact the author.

Declarations

Competing interests

The authors declare no competing interests.

Author contributions

Nan Wang and Zhi-Bo Yang constructed the theoretical scheme, Nan Wang wrote the main manuscript text, Shi-Yan Li gave some important suggestions about the calculation methods, Ting-Ting Dong prepared the Figs. 2-3, and the corresponding author Ai-Dong Zhu made the final revisions. All authors reviewed and approved the final manuscript.

Author details

¹Department of Physics, College of Science, Yanbian University, Yanji, Jilin, China. ²School of Physics, Harbin Institute of Technology, 150001 Harbin, Heilongjiang, China. ³Department of Physics, Southern University of Science and Technology, 518055 Shenzhen, China.

References

1. Soykal ÖO, Flatté ME. Strong field interactions between a nanomagnet and a photonic cavity. *Phys Rev Lett.* 2010;104:077202.
2. Huebl H, Zollitsch CW, Lotze J, Hocke F, Greifenstein M, Marx A, Gross R, Goennenwein STB. High cooperativity in coupled microwave resonator ferrimagnetic insulator hybrids. *Phys Rev Lett.* 2013;111:127003.
3. Zhang X, Zou CL, Jiang L, Tang HX. Strongly coupled magnons and cavity microwave photons. *Phys Rev Lett.* 2014;113:156401.
4. Tabuchi Y, Ishino S, Ishikawa T, Yamazaki R, Usami K, Nakamura N. Hybridizing ferromagnetic magnons and microwave photons in the quantum limit. *Phys Rev Lett.* 2014;113:083603.
5. Goryachev M, Farr WG, Creedon DL, Fan Y, Kostylev M, Tobar ME. High-cooperativity cavity QED with magnons at microwave frequencies. *Phys Rev Appl.* 2014;2:054002.
6. Cao Y, Yan P, Huebl H, Goennenwein STB, Bauer GEW. Exchange magnon-polaritons in microwave cavities. *Phys Rev B.* 2015;91:094423.
7. Bai L, Harder M, Chen YP, Fan X, Xiao JQ, Hu CM. Spin pumping in electro-dynamically coupled magnon-photon systems. *Phys Rev Lett.* 2015;114:227201.
8. Yao BM, Gui YS, Xiao Y, Guo H, Chen XS, Lu W, Chien CL, Hu CM. Theory and experiment on cavity magnon-polariton in the one-dimensional configuration. *Phys Rev B.* 2015;92:184407.
9. Lambert NJ, Haigh JA, Ferguson AJ. Identification of spin wave modes in yttrium iron garnet strongly coupled to a co-axial cavity. *J Appl Phys.* 2015;117:053910.
10. Quirion DL, Tabuchi Y, Gloppe A, Usami K, Nakamura Y. Hybrid quantum systems based on magnonics. *Appl Phys Express.* 2019;12:070101.
11. Zhang X, Zou CL, Zhu N, Marquardt F, Jiang L, Tang HX. Magnon dark modes and gradient memory. *Nat Commun.* 2015;6:8914.
12. Tabuchi Y, Ishino S, Noguchi A, Ishikawa T, Yamazaki R, Usami K, Nakamura Y. Coherent coupling between a ferromagnetic magnon and a superconducting qubit. *Science.* 2000;349:405–8.
13. Osada A, Hisatomi R, Noguchi A, Tabuchi Y, Yamazaki R, Usami K, Sadgrove M, Yalla R, Nomura M, Nakamura N. Cavity optomagnonics with spin-orbit coupled photons. *Phys Rev Lett.* 2016;116:223601.
14. Haigh JA, Nunnenkamp A, Ramsay AJ, Ferguson AJ. Triple-resonant Brillouin light scattering in magneto-optical cavities. *Phys Rev Lett.* 2016;117:133602.
15. Hisatomi R, Osada A, Tabuchi Y, Ishikawa T, Noguchi A, Yamazaki R, Usami K, Nakamura Y. Bidirectional conversion between microwave and light via ferromagnetic magnons. *Phys Rev B.* 2016;93:174427.
16. Lachance-Quirion D, Tabuchi Y, Ishino S, Noguchi A, Ishikawa T, Yamazaki R, Nakamura Y. Resolving quanta of collective spin excitations in a millimeter-sized ferromagnet. *Sci Adv.* 2017;3:e1603150.
17. Braggio C, Carugno G, Guarise M, Ortolan A, Ruoso G. Optical manipulation of a magnon-photon hybrid system. *Phys Rev Lett.* 2017;118:107205.
18. Zhang D, Luo XQ, Wang YP, Li TF, You JQ. Observation of the exceptional point in cavity magnon-polaritons. *Nat Commun.* 2017;8:1368.
19. Zhang GQ, You JQ. Higher-order exceptional point in a cavity magnonics system. *Phys Rev B.* 2019;99:054404.
20. Wang YP, Zhang GQ, Zhang DK, Li TF, Hu CM, You JQ. Bistability of cavity magnon polaritons. *Phys Rev Lett.* 2018;120:057202.
21. Hensen B et al. *Nature (London).* 2015;526:682.
22. Giustina M et al. *Phys Rev Lett.* 2015;115:250401.
23. Shalm LK et al. *Phys Rev Lett.* 2015;115:250402.
24. Bennett CH, Brassard G, Crépeau C, Jozsa R, Peres A, Wootters WK. *Phys Rev Lett.* 1993;70:1895.
25. Bouwmeester D, Pan JW, Mattle K, Eibl M, Weinfurter H, Zeilinger A. *Nature (London).* 1997;390:575.
26. Furusawa A et al. *Science.* 1998;282:706.
27. Giovannetti V, Lloyd S, Maccone L. Advances in quantum metrology. *Nat Photonics.* 2011;5:222–9.
28. Raussendorf R, Briegel HJ. A one-way quantum computer. *Phys Rev Lett.* 2001;86:5188.
29. Knill E, Laflamme R, Milburn GJ. A scheme for efficient quantum computation with linear optics. *Nature (London).* 2001;409:46.
30. Ladd TD, Jelezko F, Laflamme R, Nakamura Y, Monroe C, O'Brien JL. Quantum computers. *Nature (London).* 2010;464:45.
31. Albash T, Lidar DA. Adiabatic quantum computation. *Rev Mod Phys.* 2018;90:015002.
32. Einstein A, Podolsky B, Rosen N. Can quantum-mechanical description of physical reality be considered complete? *Phys Rev.* 1935;47:777.
33. Reid MD. Demonstration of the Einstein-Podolsky-Rosen paradox using nondegenerate parametric amplification. *Phys Rev A.* 1989;40:913.
34. Horodecki R, Horodecki P, Horodecki M, Horodecki K. Quantum entanglement. *Rev Mod Phys.* 2009;81:865.
35. Bell JS. On the Einstein Podolsky Rosen paradox. *Physics.* 1964;1:195.
36. Branciard C, Cavalcanti EG, Walborn SP, Scarani V, Wiseman HM. One-sided device-independent quantum key distribution: security, feasibility, and the connection with steering. *Phys Rev A.* 2012;85:010301(R).
37. Armstrong S, Wang M, Teh RY, Gong QH, He QY, Janousek J, Bachor HA, Reid MD, Lam PK. Multipartite Einstein-Podolsky-Rosen steering and genuine tripartite entanglement with optical networks. *Nat Phys.* 2015;11:167–72.
38. Xiang Y, Kogias I, Adesso G, He QY. Multipartite Gaussian steering: monogamy constraints and quantum cryptography applications. *Phys Rev A.* 2017;95:010101(R).
39. Kogias I, Xiang Y, He QY, Adesso G. Unconditional security of entanglement-based continuous-variable quantum secret sharing. *Phys Rev A.* 2017;95:012315.
40. Piani M, Watrous J. Necessary and sufficient quantum information characterization of Einstein-Podolsky-Rosen steering. *Phys Rev Lett.* 2015;114:060404.
41. Reid MD. Signifying quantum benchmarks for qubit teleportation and secure quantum communication using Einstein-Podolsky-Rosen steering inequalities. *Phys Rev A.* 2013;88:062338.

42. He QY, Rosales-Zárate L, Adesso G, Reid MD. Secure continuous variable teleportation and Einstein–Podolsky–Rosen steering. *Phys Rev Lett.* 2015;115:180502.
43. Chiu CY, Lambert N, Liao TL, Nori F, Li CM. No-cloning of quantum steering. *npj Quantum Inf.* 2016;2:16020.
44. Li J, Zhu SY, Agarwal GS. Magnon-photon-phonon entanglement in cavity magnomechanics. *Phys Rev Lett.* 2018;121:203601.
45. Li J, Zhu SY. Entangling two magnon modes via magnetostrictive interaction. *New J Phys.* 2019;21:085001.
46. Yu M, Shen H, Li J. Magnetostrictively induced stationary entanglement between two microwave fields. *Phys Rev Lett.* 2020;124:213604.
47. Wang N, Yang ZB, Li SY, Tong YL, Zhu AD. Nonreciprocal transmission and asymmetric entanglement induced by magnetostriction in a cavity magnomechanical system. *Eur Phys J Plus.* 2022;137:1–10.
48. Zhang ZD, Scully MO, Agarwal GS. Quantum entanglement between two magnon modes via Kerr nonlinearity driven far from equilibrium. *Phys Rev Res.* 2019;1:023021.
49. Kittel C. On the theory of ferromagnetic resonance absorption. *Phys Rev.* 1948;73:155.
50. Yang ZB, Wu WJ, Li J, Wang YP, You JQ. Steady-entangled-state generation via the cross-Kerr effect in a ferrimagnetic crystal. *Phys Rev A.* 2022;106:012419.
51. Yuan HY, Zheng SS, Ficek Z, He QY, Yung MH. Enhancement of magnon-magnon entanglement inside a cavity. *Phys Rev B.* 2020;101:014419.
52. Zheng SS, Sun FX, Yuan HY, Ficek Z, Gong QH, He QY. Enhanced entanglement and asymmetric EPR steering between magnons. *Sci China, Phys Mech Astron.* 2021;64:210311.
53. Yang ZB, Liu XD, Yin XY, Ming Y, Liu HY, Yang RC. Controlling stationary one-way quantum steering in cavity magnonics. *Phys Rev Appl.* 2021;15:024042.
54. Guan SY, Wang HF, Yi X. Cooperative-effect-induced one-way steering in open cavity magnonics. *npj Quantum Inf.* 2022;8:1–9.
55. Li X, Voss PL, Sharping JE, Kumar P. Optical-fiber source of polarization-entangled photons in the 1550 nm telecom band. *Phys Rev Lett.* 2005;94:053601.
56. Yang ZB, Liu HY, Yang RC. Manipulation of one-way Gaussian steering via quantum correlated microwave fields. *Ann Phys.* 2021;533:2100156.
57. Li J, Zhu SY, Agarwal GS. Squeezed states of magnons and phonons in cavity magnomechanics. *Phys Rev A.* 2019;99:021801(R).
58. Nair JMP, Agarwal GS. Deterministic quantum entanglement between macroscopic ferrite samples. *Appl Phys Lett.* 2020;117:084001.
59. Zhang XF, Zou CL, Jiang L, Tang HX. Cavity magnomechanics. *Sci Adv.* 2016;2:e1501286.
60. Vitali D, Gigan S, Ferreira A, Bohm HR, Tombesi P, Guerreiro A, Vedral V, Zeilinger A, Aspelmeyer M. Optomechanical entanglement between a movable mirror and a cavity field. *Phys Rev Lett.* 2007;98:030405.
61. Eisert J. Ph D thesis. Potsdam: University of Potsdam; 2001.
62. Vidal G, Werner RF. Computable measure of entanglement. *Phys Rev A.* 2002;65:032314.
63. Adesso G, Serafini A, Illuminati F. Extremal entanglement and mixedness in continuous variable systems. *Phys Rev A.* 2004;70:022318.
64. Plenio MB. Logarithmic negativity: a full entanglement monotone that is not convex. *Phys Rev Lett.* 2005;95:090503.
65. Hidki A, Ren YL, Lakhfif A, Qars JE, Nassik M. Enhanced maximum entanglement between two microwave fields in the cavity magnomechanics with an optical parametric amplifier. *Phys Lett A.* 2023;463:128667.
66. Lifshitz EM, Pitaevskii LP. *Statistical physics: theory of the condensate state, part 2.* revised ed. Oxford: ButterworthHeinemann; 1980.
67. Fetter AL, Walecka JD. *Quantum theory of many particle systems.* Mineola: Dover; 2003.
68. Kogias I, Lee AR, Ragy S, Adesso G. Quantification of Gaussian quantum steering. *Phys Rev Lett.* 2015;114:060403.
69. Zhang GQ, Wang YP, You JQ. Theory of the magnon Kerr effect in cavity magnonics. *Sci China, Phys Mech Astron.* 2019;62:987511.
70. Gardiner CW. Inhibition of atomic phase decays by squeezed light: a direct effect of squeezing. *Phys Rev Lett.* 1986;56:1917.
71. Palomaki TA, Teufel JD, Simmonds RW, Lehnert KW. Entangling mechanical motion with microwave fields. *Science.* 2013;342:710.

Publisher's Note

Springer Nature remains neutral with regard to jurisdictional claims in published maps and institutional affiliations.